Title
Osteoblast-derived FGF9 regulates skeletal homeostasis

Authors
Wang, Liping
Roth, Theresa
Abbott, Marcia
et al.

Publication Date
2017-05-01

DOI
10.1016/j.bone.2016.12.005

Peer reviewed

Published in final edited form as:
Bone. 2017 May ; 98: 18–25. doi:10.1016/j.bone.2016.12.005.

Osteoblast-derived FGF9 regulates skeletal homeostasis

Liping Wang[a,b], **Theresa Roth**[a], **Marcia Abbott**[a,1], **Linh Ho**[a], **Lalita Wattanachanya**[a,c,d], **Robert A. Nissenson**[a,b,*]

[a]Endocrine Unit, VA Medical Center, San Francisco, CA, USA

[b]Department of Medicine, University of California, San Francisco, CA, USA

[c]Division of Endocrinology and Metabolism, Department of Medicine, Faculty of Medicine, Chulalongkorn University, Thai Red Cross Society, Bangkok, Thailand

[d]King Chulalongkorn Memorial Hospital, Bangkok, Thailand

Abstract

FGF9 has complex and important roles in skeletal development and repair. We have previously observed that Fgf9 expression in osteoblasts (OBs) is regulated by G protein signaling and therefore the present study was done to determine whether OB-derived FGF9 was important in skeletal homeostasis. To directly test this idea, we deleted functional expression of Fgf9 gene in OBs using a 2.3 kb collagen type I promoter-driven Cre transgenic mouse line ($Fgf9^{OB-/-}$). Both Fgf9 knockout ($Fgf9^{OB-/-}$) and the Fgf9 floxed littermates ($Fgf9^{fl/fl}$) mice were fully backcrossed and maintained in an FBV/N background. Three month old $Fgf9^{OB-/-}$ mice displayed a significant decrease in cancellous bone and bone formation in the distal femur and a significant decrease in cortical thickness at the TFJ. Strikingly, female $Fgf9^{OB-/-}$ mice did not display altered bone mass. Continuous treatment of mouse BMSCs with exogenous FGF9 inhibited mouse BMSC mineralization while acute treatment increased the proliferation of progenitors, an effect requiring the activation of Akt1. Our results suggest that mature OBs are an important source of FGF9, positively regulating skeletal homeostasis in male mice. Osteoblast-derived FGF9 may serve a paracrine role to maintain the osteogenic progenitor cell population through activation of Akt signaling.

Keywords

Bone formation; FGF9; Osteoblasts; Akt; Stem cells

*Corresponding author at: VA Medical Center (111 N-MB), 1700 Owens St. Room 370, San Francisco, CA 94158, USA. Robert.Nissenson@ucsf.edu (R.A. Nissenson).
[1]Current address: Chapman University, One University Drive, Orange, CA.

Supplementary data to this article can be found online at http://dx.doi.org/10.1016/j.bone.2016.12.005.

Disclosure statement
All authors state that they have no conflicts of interest.

1. Introduction

The adult skeleton is a dynamic organ that supports body weight and maintains mineral homeostasis through continuous bone remodeling at bone surfaces. This process requires coordinated cellular activities between osteoclast and osteoblast lineage cells, in which osteoblasts are responsible for regulating osteoclasts and depositing bone matrix through perceiving mechanical and biochemical cues, such as hormones and growth factors within bone marrow microenvironment [1]. Parathyroid hormone (PTH) promotes osteoblast function and has emerged as a major approach for clinical treatment of osteoporosis because of its anabolic effects. PTH activates the G_s-cyclic AMP signaling pathway by acting on the PTH/PTHrP receptor 1 (PTHR1) in osteoblasts. By assessing the transcriptome of maturing osteoblasts expressing a G_s-activating engineered receptor (Rs1) [2,3], we found that fibroblast growth factor 9 (Fgf9) was significantly down-regulated by G_s signaling, suggesting a possible role for osteoblast-derived FGF9 in regulating bone homeostasis [4].

Signaling pathways initiated by the FGF ligand and FGF receptor (FGFR) system are crucial for various cellular processes, including proliferation, differentiation and survival [5]. The functional link between FGF signaling and vertebral limb development has been extensively studied [6–9]. Signaling through FGFR1 and FGFR2 involve bones arise by intramembraneous ossification and mutations of FGFR1 and 2 principally induce craniosynostosis and facial abnormalities [10,11]. Signaling through FGFR3 principally affects bones that arise by endochondral ossification and mutations in FGR3 cause several types of the human skeletal dysplasias including achondroplasia, hypochondroplasia, thanaachondroplasia, and severe achondroplasia [11].

FGF9 expression is localized to perichondrium/periosteum, trabecular bone, and the mesenchyme surrounding developing bones [12]. FGF9 can interact with multiple FGFRs, but has the highest affinity for FGFR3 [6,13,14]. FGF9 is reported to have complex and important roles in skeletal development and repair [10,15–18]. For instance, FGF9 null mice exhibit a lethal phenotype with a limb developmental defect that is similar to achondroplasia in human [12]. Haploinsufficiency of Fgf9 represses bone fracture repair [17]. Conditional over-expression of FGF9 in cartilage caused an inhibitory phenotype of chondrocyte terminal differentiation with less subchondral bone formation [6]. In contrast to its diverse activities in development and physiology, the roles of the FGF9 in bone homeostasis are still unclear due to functional and structural redundancy and the similar receptor specificity across FGF ligands [5,19].

In this study, we addressed the physiological role of osteoblast-derived FGF9 by deleting its expression in maturing osteoblasts using the 2.3 kb collagen type I promoter driven Cre recombinase. We found that osteoblast-derived FGF9 has a sex dimorphic (male-specific) effect on adult mouse skeleton associated with an increase in osteoblast progenitor cell proliferation and suppression of osteoblast differentiation.

2. Materials and methods

2.1. Animals

All transgenic mouse studies were approved by and performed in accordance with the Institutional Animal Care and Use Committees at the San Francisco Veterans Affairs Medical Center and at the University of California, San Francisco.

The transgenic mice with Fgf9 gene specifically depleted in osteoblasts were generated by crossing the male transgenic mice that heterogeneously harbor the Cre recombinase gene (Cre) driven by a 2.3 kb type 1 collagen promoter [STOCK Tg(Col1a1-Cre)2Bek/Mmucd, MMRRC] with the female $Fgf9^{flox/flox}$ mice (generously provided by Dr. Fen Wang, Texas A&M Health Science Center) [20]. To minimize the unnecessary genetic effects on bone metabolism, we backcrossed all the mice to a FVB/N background. The homozygous $Fgf9^{flox/flox}$ mice in a FVB/N background were bred by crossing the $Fgf9^{flox/flox}$ chimeras with the wild type FVB/N mice for 10 generations (Fig. 1A). The average litter size for a FVB/N mouse breeding pair was between 8 and 10 pups in this study. Our breeding strategy has resulted in that the offspring of each litter mice had 50% chance to be osteoblast conditional knockout mice (Co l1 (2.3)-Cre; $Fgf9^{flox/flox}$)($Fgf9^{OB-/-}$) and the other 50% mice were likely to be $Fgf9^{flox/flox}$, which served as littermate controls ($Fgf9^{fl/fl}$).

All mice were group-housed at 5 mice per plastic cage, maintained in a humidity and temperature controlled facility with a 12/12 h light/dark cycle, and fed with food and water ad libitum. At the termination of this study, 12 week old mice were euthanized and both femurs and tibiae were subjected to skeletal phenotype assessment as indicated below. To study bone formation and mineralization, mice were injected with 20 mg/kg of calcein (Sigma-Aldrich, St Louis, MO, USA) 21 and 7 days before euthanasia and with 15 mg/kg of demeclocycline (Sigma-Aldrich) 2 days before euthanasia.

2.2. Analysis of bone formation

Mice were euthanized and femurs and tibiae were removed and dissected free from surrounding musculature. Bones were fixed in 10% neutral-buffered formalin for 48 h at 4 °C and then stored in 70% ethanol before μCT and histomorphometry. The distal femurs and tibio-fibular junction (TFJ) were scanned using a Scanco VivaCT-50 μCT system (Bruttisellen, Switzerland). All μCT images were obtained using an X-ray energy of 55 kV with a voxel size of 10.5 μm and integration time of 1000 ms. The cancellous region of interest (ROI) was at a distance of 0.10 to 1.35 mm from the primary spongiosa. The cancellous ROI was assessed in distal femurs using a global thresholding protocol with segmentation values of 0.8/1/270. Quantitative assessment of diaphyseal cortex at TFJ was conducted using data from 40 slices (0.42 mm) using a global thresholding protocol with segmentation values of 0.8/1/365.

2.3. Histomorphometry

Following μCT analysis, the un-decalcified femurs and tibiae were embedded in methyl methacrylate and then sectioned with Jung 2065 and 2165 microtomes (Leica, 145 Bannockburn, IL, USA). Assessment of bone formation activity at cancellous bone surfaces

was performed on the unstained, 10-μm longitudinal sections from the left femur. Five-μm sections of distal femur bones were also processed for Von Kossa/Trichrome staining as previously described for static histomorphometry [21]. Assessment of cortical bone was performed on 10-μm transverse sections at TFJ. Before histomorphometry, mosaic-tiled images of distal femur and TFJ were acquired at ×200 magnification with a Zeiss Axioplan Imager M1 microscope (Carl Zeiss MicroImaging, Thornwood, NY, USA) fitted with a motorized stage. The tiled images were stitched and converted to a single image using the Axiovision software (Carl Zeiss MicroImaGing) prior to blinded analyses being performed using image-analysis software (Bioquant Image Analysis Corp., Nashville, TN, USA). Cancellous bone was assessed in the region 100 μm from the lowest point on the growth plate, extending 1 mm down the metaphysis. To measure the number of osteoclast per bone surface in the trabecular bone, 5-μm longitudinal sections from the distal femur were stained for tartrate resistant acid phosphatase (TRAP) [22–24]. The dynamic indices of bone formation within the same region that were measured on 10-μm sections and percent mineralizing surface (MS/BS), mineral apposition rate (MAR), and surface-based bone-formation rate (BFR/BS) were determined by Bioquant OSTEO software.

2.4. RNA extraction and RT-qPCR

Both femur and tibia were isolated immediately after animals were euthanized. The epiphyses were then removed and bone morrow was flushed with PBS. The diaphyses were kept frozen in liquid nitrogen until processing. Frozen tissues were pulverized using a biopulverizer (Biospec Products, Inc., Bartlesville, OK, USA), followed by RNA extraction using RNA STAT60 (Tel-Test, Inc., Friendswood, TX, USA) and subsequent purification using Micro-to-Midi Total RNA Purification Kit (Invitrogen, Carlsbad, CA, USA). cDNA was synthesized using TaqMan Reverse Transcription Reagents (Applied Biosystems, Inc., Foster City, CA, USA) and random hexamer primers according to the recommendations of the manufacturer. Gene amplification was measured with SYBR Green using the ABI Prism ViiA™ 7 real-time PCR System (Waltham, MA, USA). Analysis was carried out using the ViiA™ 7 software supplied with the thermocycler. The sequences of the primer sets have been published previously [4,23,25]. The target gene expression was displayed normalized to GAPDH.

2.5. Serum chemistry

Before euthanizing the mice, blood was collected from the abdominal inferior vein when mice were under isoflurane inhalation anesthesia and then processed in MicroTainer serum separator tubes (BD Biosciences, San Jose, CA, USA). Serum procollagen type I amino-terminal propeptide (PINP) and serum pyridinoline (PYD) measurements were carried out using the rat/mouse PINP EIA Kit AC-33F1 from Immunodiagnostic Systems (Scottsdale, AZ, USA) and the Metra Biosystems Serum PYD Kit 8019 (Metra Biosystems Inc., Santa Clara, CA, USA) according to manufacturers' directions.

2.6. Bone marrow stromal cell culture and mineralization in vitro

Briefly, the bone marrow plugs from 8 to 10 week old wild type FVB/N mice were flushed out from both femurs and tibiae and cultured in primary culture medium, alpha modification of Eagle's medium (α-MEM; Thermo Scientific) supplemented with 10% fetal bovine

serum (HyClone), 100 U/ml penicillin, 100 μg/ml streptomycin (Invitrogen), and 0.25 μg/ml Fungizone [26]. Bone marrow stromal cells (BMSCs) were plated into 6-well plates at a density of 1.8–2.3 × 10^6 cells/well. Cells were incubated in a humidified atmosphere of 5% CO_2 at 37 °C. On day seven, 50 μg/ml ascorbic acid (Sigma-Aldrich) and 3 mM β-glycerol phosphate (Sigma-Aldrich) were added to the primary culture media to induce osteoblastic differentiation. Media was changed every 2–3 days. To assess mineralization, 2% silver nitrate solution (Sigma-Aldrich) was added to cell culture dishes on day 21 for Von Kossa (VK) staining and UV-crosslinked for 10 min. Stained cultures were scanned and quantified using Improvision Openlab software version 5.0.2.

2.7. Cell proliferation

Effect of FGF9 on mouse BMSC proliferation was determined by measuring BrdU incorporation using a Cell Proliferation ELISA kit (Roche Applied Science, Indianapolis, IN) [23]. Briefly, mouse BMSCs were plated onto 96-well plates at a seeding density of 1 × 10^4 cells/well in primary culture media. On day 3, 1–10 ng/ml recombinant mouse FGF9 (R&D Systems, INC, Minneapolis, MN) was added to the media for 24 h, and BrdU was added 4 h prior to the assay. The incorporated BrdU in each culture was quantified according to the manufacturer's instruction. The results of this assay were confirmed by repeating the experiment three times.

2.8. Protein extraction and immunoblotting

The wild type BMSCs at confluence were treated with 5 ng/ml FGF9 for 24 h. FGF9 solution was prepared in the osteogenic medium, in which the fetal bovine serum (FBS) was omitted to eliminate the effect of serum components on the phosphorylation of Akt and Akt1. Whole cells protein lysates were prepared using RIPA buffer (50 mM sodium chloride, 1.0% NP-40, 0.5% sodium deoxycholate, 0.1% SDS (sodium dodecyl sulfate), 50 mM Tris, pH 8.0) plus protease and phosphatase inhibitor cocktail (Thermo Fisher Scientific) and measured the concentrations using BCA assay (Thermo Fisher Scientific). Protein samples (10–15 μg/lane) were resolved by SDS-PAGE (10% separating gel), transferred to PVDF membranes, and subjected to immunoblot analysis with specific antibodies against Akt; Akt1, phosphorylated Akt; and phosphorylated Akt1 (Cell Signaling) at the dilution of 1:1000. Detection was made by enhanced chemiluminescence (ECL) using SuperSignal West Dura Extended Duration Substrate (Thermo Fisher Scientific). Data was captured using Fujifilm LAS 4000 (Fuji Medical Systems, USA).

2.9. Statistical analysis

Statistical significance was ascertained by a two-tailed Student's *t*-test or, where indicated, by two-way ANOVA. $\alpha \leq 0.05$ was considered significant.

3. Results

3.1. Loss of Fgf9 in osteoblasts has no effect on bone growth

FGF9 participates in multiple steps of endochondral ossification to regulate skeletal development in the proximal limb [6]. The Fgf9 null mice have rhizomelic limb shortening, initiated at the earliest stages of skeletal growth. However, specific knockout Fgf9 gene in

osteoblasts (OBs) did not replicate the skeletal phenotypes in Fgf9 null mice [12]. We did not observe a significant change of body weights up to 3 months of age (Fgf9 $^{fl/fl}$ vs. Fgf9 $^{OB-/-}$: male, 24.13 ± 0.59 vs. 23.3 ± 0.62 g; female, 18.42 ± 0.27 vs. 17.8 ± 0.97 g).

3.2. Loss of Fgf9 in osteoblasts decreases cancellous bone formation in adult male bones

To test the specificity of Cre gene expression, we bred the Co l1 (2.3)-Cre mice with a line of Rosa tomato red mice (generously provided by Dr. Ann Zovein, University of California San Francisco, CA) (Fig. 1B). The Cre recombinase is demonstrated to be expressed in OBs and osteocytes (OCTs) in adult Coll (2.3)-Cre; td/Tomato Red mice (Fig. 1B). To test the efficiency of Fgf9 deletion in Fgf9$^{OB-/-}$ mice, we also performed reverse transcription end point PCR on RNA extracted from long bones and demonstrated that Fgf9 gene was successfully excised by Cre recombinase (Fig. 1C) [20] and as expected, the conditional Cre-loxp recombination dramatically decreased Fgf9 mRNA level in both male and female Fgf9$^{OB-/-}$ mice (Fig. 1D).

MicroCT assessment demonstrated that Fgf9 deletion led to a dramatic decrease in cancellous bone fractional volume (BV/TV) at distal femur in male, but not female, Fgf9 $^{OB-/-}$ mice (Fig. 2A and Table 1). The decrease was mainly associated with a significant decrease in trabecular thickness (Tb.Th) ($p < 0.001$) and an increase in trabecular separation (Tb.Sp) (Table. 1). In contrast, Fgf9 deficiency did not change trabecular number (Tb.N) (Table. 1). The effects of Fgf9 gene deletion on adult mouse bones were also evaluated by histomorphometry. The 3 month old male Fgf9 $^{OB-/-}$ mice showed a significant decrease in cancellous BV/TV and Tb.N, and a significant increase in Tb.Sp, compared to the age and sex-matched Fgf9 $^{fl/fl}$ mice (Fig. 2B). However, the female transgenic mice displayed no change in BV/TV, Tb.Th, Tb.N, and Tb.Sp at the distal femur (Fig. 2B). The osteoblasts sitting at the trabecular surface (N.Ob/BS) was also counted. It was found that N.Ob/BS was significantly lower in the male but not in the female Fgf9 $^{fl/fl}$ mice, compared to the age-matched controls (Supplemental Fig. 1A).

To reveal the mechanism by which the loss of Fgf9 in osteoblasts led to decreased cancellous factional bone volume, we performed dynamic histomorphometry on the same bones (Fig. 2C). A sexual dimorphic response of bone formation to the Fgf9 deletion in osteoblasts was also observed at the distal femur by measuring fluorescence labeled trabecular surfaces (Fig. 2C). Male Fgf9 $^{OB-/-}$ mice displayed decreased MS/BS and BFR. However, trabecular MAR was not altered in male Fgf9 $^{OB-/-}$ mice. In contrast, there were no differences seen in the parameters of dynamic histomorphometry between female Fgf9 $^{OB-/-}$ mice and sex matched littermate control mice (Fig. 2C).

3.3. Loss of Fgf9 in osteoblasts decreases cortical bone formation in adult male bones

The cortical bone shell is a key determinant of bone strength and fracture risk and thins rapidly with age [27,28]. Effects of the conditional knockout of Fgf9 on cortical bone volume, cortical bone thickness, and bone marrow area were assessed at the TFJ by μCT (Fig. 3A and Table 1). In male mice, there was no difference in tissue volume between the knockout and the littermate control mice. However, the Fgf9 deletion resulted in a slight and

statistically significant decrease in bone volume and cortical bone thickness (Ct.Th). There were no significant differences observed between female control and transgenic mice (Table 1). The changes in cortical bone were further confirmed by histological analysis of the TFJ in Fgf9$^{OB-/-}$ (Fig. 3B). In males, loss of Fgf9 in osteoblasts did not affect the cortical periosteal perimeter. The endosteal perimeter and bone marrow area were significantly greater while cortical thickness was significantly smaller at the TFJ in male Fgf9$^{OB-/-}$ mice (Fig. 3B). This result demonstrates that the loss of bone that occurred at the TFJ was mainly at the endosteal surface. The decreased bone formation at both periosteal and endosteal surfaces of the TFJ was mainly due to the decreased mineralizing surface in male Fgf9 $^{OB-/-}$. There were no significant changes in any of the cortical parameters in female mice (Fig. 3C). In addition, it has been found that the Ps.BFR is decreased in Fgf9$^{OB-/-}$ male mice without any significant changes in periosteal perimeter (Ps.Pm) (Fig. 3B and C). The mice used in this study were at age of 3 months and by then the peak bone mass has already been established [29]. Our result suggests that the source of FGF9 from mature osteoblasts possibly does not impact the cortical bone accrual during growth but may affect the cortical bone expansion during aging.

3.4. Endogenous Fgf9 restrains the function of mature osteoblasts

We examined the effects of Fgf9 deletion on the expression of genes in the femoral diaphysis. We observed no change in the expression of the early osteogenic marker genes, such as *Osx* and *Runx2*. Surprisingly, *collagen type 1 (Col1)*, *osteoclacin (Ocn)*, and *Dmp1* mRNA expression was significantly higher in male Fgf9$^{OB-/-}$, compared to age-matched Fgf9 $^{fl/fl}$ mice. There were no significant differences observed between female transgenic and control mice, in regards to gene expression (Fig. 4). It has been reported that Fgf9 is important for promoting skeletal vascularization and global Fgf9 null mice displayed delayed osteogenesis due to defects in angiogenesis [12]. However, we did not detect a significant change in *pecam1* mRNA expression in the Fgf9$^{OB-/-}$ mice (data not shown).

3.5. Bone resorption in adult Fgf9 $^{OB-/-}$ mouse bone was not altered

In a previous study, Fgf9 null mice were found to display a reduction in osteoclast numbers in the perichondrium and primary spongiosa of the developing long bones [12]. To examine if Fgf9 deficiency in osteoblasts affects osteoclastogenesis in adult skeleton, we performed TRAP staining and found that the specific deletion of Fgf9 in osteoblasts did not alter the number of osteoclasts (N.Oc/BS) within the distal femur (Fig. 5). Consistent with this finding, serum PYD was not changed, either (Fig. 5). Although the levels of *Opg* and *Rankl* mRNA were increased in males (data not shown), the ratio of OPG/RANKL was not significantly altered by deleting Fgf9 (Fig. 5).

3.6. Exogenous FGF9 stimulates proliferation of BMSCs

We demonstrated that Fgf9 $^{OB-/-}$ mice displayed an osteoblastic phenotype, in which deletion of Fgf9 in osteoblasts led to a low bone mass due to a decreased bone formation rate in male skeleton. We have carried out additional studies to determine whether there is a cell autonomous autocrine role for FGF9 in promoting osteogenesis. We found that bone marrow stromal cells derived from male Fgf9 $^{OB-/-}$ mice displayed osteogenic differentiation that was comparable to that seen in cultures from WT mice (Supplemental

Fig. 1B). These findings suggest that osteoblast derived FGF9 promotes osteogenesis through paracrine effects on osteoprogenitors. To test this hypothesis, we cultured BMSCs from wild type mice and the effect of exogenous FGF9 on BMSC proliferation was examined using a BrdU incorporation assay. It was found that treatment with rmFGF9 for 24 h significantly increased proliferation in both male and female BMSCs in a dose dependent manner (Fig. 6A). Strikingly, BMSCs from male mice were more responsive to FGF9 than were BMSCs from female mice. At a dose of 5 ng/ml rmFGF9, there was a 209% ($p < 0.01$) increase in BrdU labelled male cells and a 76% ($p < 0.05$) increase in BrdU labeled female cells, when compared to sex matched, vehicle treated control cells (Fig. 6A).

We have examined the expression levels of FGFR3 in both bone marrow progenitors (PCs) and mature osteoblasts (OBs) because FGF9 has the highest affinity for FGFR3 [6,13,14]. It was found that the expression level of FGFR3 mRNA was much higher in mature OBs regardless of gender and genotype (supplemental Fig. 2A). We also assessed whether exogenous FGF9 would produce anabolic effects in maturing OBs due to their high level of expression of FGFR3. In this study, the BMSCs from male and female wild type mice were cultured separately. FGF9 at a dose of 5 ng/ml was administered to OBs from day 14 to day 21 post culture, mRNA levels of the osteogenic marker genes including osterix, Runx2, alkaline phosphatase, type 1 collagen and osteocalcin were measured using real time PCR. It was found that mRNA levels of these bone marker genes were decreased by FGF9 treatment regardless of gender (Supplemental Fig. 2B and C).

3.7. FGF9 stimulates proliferation of BMSCs through Akt1 signaling pathway

Inhibition of Akt activity by adding the Akt inhibitor MK-2206 (1 μM) completely eliminated the stimulatory effect of FGF9 on osteoblast precursor proliferation in vitro (Fig. 6B). Additionally, levels of Akt1and phosphorylated Akt1 in the confluent BMSCs treated with FGF9 were measured by western blot. It was found that exogenous FGF9 stimulated BMSC proliferation by mainly increasing phosphorylation of Akt1 (Fig. 6C), a result in line with the previous finding that loss of Akt1 was shown to be deleterious to osteoblast precursor development, leading to lower bone mass in male (but not female) mice [30].

4. Discussion

FGF9 is critical for skeletal development [6–9]. It has been reported that FGF9 is expressed in the proximity of the developing skeleton and that Fgf9 null mice exhibited a limb phenotype with rhizomelia [12]. FGF9 is expressed at low levels in osteoprogenitor cells, but is highly expressed in mature osteoblasts [31]. The physiological role of osteoblast-derived FGF9 in skeletal homeostasis is unknown. Our results show that deletion of Fgf9 in osteoblasts led to a significant decrease in both cancellous and cortical bone in young adult male mice. Surprisingly, the specific deletion of Fgf9 had no such effect in female mice. We have previously observed that Fgf9 expression in osteoblasts is regulated by G protein signaling [4]. Activation of G_s signaling or increasing intracellular level of cAMP, both conditions producing strong bone formation [2,3], down-regulated the expression of Fgf9 in mature osteoblasts. This led us to hypothesize that osteoblast-derived FGF9 might play a negative role in skeletal anabolism. However, deletion of Fgf9 in osteoblasts

resulted in an osteopenic phenotype, as evidenced by a decreased trabecular bone fractional volume with decreased bone formation at trabecular bone surfaces in male $Fgf9^{OB-/-}$ mice. Histomorphometry also demonstrated that FGF9 deficiency resulted in a decrease in number of OBs and mineralized surface (MS/BS) but had no effect on MAR at the distal femur, suggesting that deletion of FGF9 in osteoblasts might not affect the speed of mineralization, but the number of osteoblasts, at the trabecular surface. In the diaphysis of long bones (where mature osteoblasts and osteocytes are the dominant osteoblast lineage cell types) loss of Fgf9 led to increased expression of markers of mature osteoblasts, including Ocn, Dmp1, and Col1. However, the male $Fgf9^{OB-/-}$ mice exhibited a decreased cortical bone thickness with a decreased cortical bone formation rate. Collectively, these findings suggest that mature osteoblasts serve as an important source of FGF9 and that secreted FGF9 regulates bone formation in adult male mice in a cell non-autonomous manner.

FGFs including FGF9 comprise the most common subfamily that transduces signals through FGFR tyrosine kinases. These polypeptides can be retained in the extracellular matrix in the vicinity of their secreting cells and act as autocrine and/paracrine factors [32,33]. In previous studies, exogenous FGF9 has been demonstrated to be pro-osteogenic and to facilitate bone regeneration [17,18]. Recently, FGF9 has been found to induce osteoblast proliferation and new bone formation in a bone organ assay [34]. In the present study, we demonstrated that exogenous FGF9 stimulates bone marrow stromal cell proliferation in a dose dependent manner, a finding similar to that of Lu et al. [35]. These findings support the hypothesis that osteoblast secreted FGF9 serves as a paracrine role to stimulate osteogenesis of bone marrow skeletal stem cells to maintain bone homeostasis. Akt1 deficiency is reported to decrease bone mass and formation [30,36]. FGF9 has been demonstrated to activate Akt pathways to stimulate steroidogenesis in mouse Leydig cells [37]. Akt1 is the major isoform in bone cells and acts to suppress osteoblast apoptosis [36]. In the present study, we demonstrated that FGF9 stimulates the proliferation of BMSCs by activating Akt1.

It is not clear why loss of Fgf9 in osteoblasts resulted in significant bone loss in male mice while not affecting the female skeleton. Available evidence suggests that there is a collaborative interaction between FGF9 and the actions of androgens on bone [30,38,39]. Firstly, FGF9 has functions related to sex domination in addition to bone formation. Mice globally lacking Fgf9 display male-to-female sex reversal [40]. Secondly, androgens promote proliferation of osteoblast progenitors and differentiation, in part, through PI3-kinase-Akt signaling pathway [30,41]. Of interest in this regard, global haploinsufficiency of Akt1 in mice also induced a decrease in femoral bone mass that was seen in males but not females [30]. Thirdly, we have demonstrated that FGF9 stimulates the proliferation of BMSCs by activating Akt1. Finally, androgens have potent effects on osteoblast formation. While androgens maintain trabecular bone mass and integrity, they favor periosteal bone formation in men [42]. These findings are consistent with the bone phenotype of FGF9 conditional knockout mice, in which deletion of Fgf9 reduced cortical bone by decreasing both periosteal and cancellous bone formation. Collectively, the growth factor, FGF9 may serve as a mediator of bone anabolic signaling of androgen/Akt1 in osteoblasts.

The effects of FGF9 on osteoblasts and progenitors are complex. In addition to delivering a mitogenic signal in a variety of cells, FGF9 is also involved in cell differentiation, motility,

and survival [43]. Experiments have suggested that FGF9 serves as an endogenous inhibitor of chondrocyte differentiation [6,44]. However, the role of FGF9 on the differentiation of OBs is not clear. FGF9 is known to signal mainly through FGFR3 in bone [13]. In this study, we found that the expression levels of FGFR3 were higher in mature OBs than bone marrow progenitor cells, independent of gender and genomic difference (Supplemental Fig. 2A) and that addition of FGF9 inhibited the expression of osteogenic marker genes in both male and female mature OBs (Supplemental Fig. 2B and C). Our results demonstrate that exposure of mature OBs to FGF9 does not elicit an "anabolic" response and that the observed difference in the effects of FGF9 on bone progenitor cells and mature osteoblasts is not likely related to the levels of FGFR3. A recent study has demonstrated that an activating mutation of FGFR3 in osteoblasts does not produce any obvious bone phenotype [45], supporting our conclusion. The seemingly inconsistent results between the Fgf9 $^{OB-/-}$ mice and these in vitro cell experiments may be due to functional redundancy between FGF ligands [5,11]. Fgf9 belongs to the canonical Fgf subfamily, Fgf9/16/20 (5). Canonical FGFs mediate biological response by binding to and activating FGFRs. Although each canonical FGF has distinct receptor binding specificity, each member of an FGF subfamily has similar receptor specificity [19]. The specific role of these receptors in mediating responses to FGF9 in bone remains to be elucidated. Given its role in fracture regeneration [17] and in diseases such as oncogenesis [46] and tumor metastasis [34,47,48], FGF9 and its signaling pathways are attractive targets for therapy.

In conclusion, our results suggest that mature osteoblasts are a possibly important source of FGF9, positively regulating skeletal homeostasis in male mice. Osteoblast-derived FGF9 may serve a paracrine role to maintain the osteogenic progenitor cell population through activation of Akt1 signaling.

Supplementary Material

Refer to Web version on PubMed Central for supplementary material.

Acknowledgments

Authors would like to thank San Francisco VA Medical Center (SF VAMC) Bone Core for its technical assistance. This work was supported by the Department of Veterans Affairs (Merit Review grant 1I01BX001496) to RAN and by NIH grant 1 P30 AR066262.

References

[1]. Mackie EJ, Osteoblasts: novel roles in orchestration of skeletal architecture, Int. J. Biochem. Cell Biol35 (9) (2003) 1301–1305. [PubMed: 12798343]

[2]. Hsiao EC, Boudignon BM, Halloran BP, Nissenson RA, Conklin BR, Gs G protein-coupled receptor signaling in osteoblasts elicits age-dependent effects on bone formation, J. Bone Miner. Res25 (3) (2010) 584–593. [PubMed: 20200944]

[3]. Hsiao EC, Millard SM, Louie A, Huang Y, Conklin BR, Nissenson RA, Ligand-mediated activation of an engineered gs g protein-coupled receptor in osteoblasts increases trabecular bone formation, Mol. Endocrinol24 (3) (2010) 621–631. [PubMed: 20150184]

[4]. Wattanachanya L, Wang L, Millard SM, Lu WD, O'Carroll D, Hsiao EC, Conklin BR, Nissenson RA, Assessing the osteoblast transcriptome in a model of enhanced bone formation due to

constitutive Gs-G protein signaling in osteoblasts, Exp. Cell Res333 (2) (2015) 289–302. [PubMed: 25704759]

[5]. Itoh N, Ornitz DM, Functional evolutionary history of the mouse Fgf gene family, Dev. Dyn237 (1) (2008) 18–27. [PubMed: 18058912]

[6]. Garofalo S, Kliger-Spatz M, Cooke JL, Wolstin O, Lunstrum GP, Moshkovitz SM, Horton WA, Yayon A, Skeletal dysplasia and defective chondrocyte differentiation by targeted overexpression of fibroblast growth factor 9 in transgenic mice, J. Bone Miner. Res14 (11) (1999) 1909–1915. [PubMed: 10571691]

[7]. Shiang R, Thompson LM, Zhu YZ, Church DM, Fielder TJ, Bocian M, Winokur ST, Wasmuth JJ, Mutations in the transmembrane domain of FGFR3 cause the most common genetic form of dwarfism, achondroplasia, Cell78 (2) (1994) 335–342. [PubMed: 7913883]

[8]. Tavormina PL, Shiang R, Thompson LM, Zhu YZ, Wilkin DJ, Lachman RS, Wilcox WR, Rimoin DL, Cohn DH, Wasmuth JJ, Thanatophoric dysplasia (types I and II) caused by distinct mutations in fibroblast growth factor receptor 3, Nat. Genet9 (3) (1995) 321–328. [PubMed: 7773297]

[9]. Horton WA, Fibroblast growth factor receptor 3 and the human chondrodysplasias, Curr. Opin. Pediatr9 (4) (1997) 437–442. [PubMed: 9300204]

[10]. Deng C, Wynshaw-Boris A, Zhou F, Kuo A, Leder P, Fibroblast growth factor receptor 3 is a negative regulator of bone growth, Cell84 (6) (1996) 911–921. [PubMed: 8601314]

[11]. Ornitz DM, Marie PJ, FGF signaling pathways in endochondral and intramembranous bone development and human genetic disease, Genes Dev. 16 (12) (2002) 1446–1465. [PubMed: 12080084]

[12]. Hung IH, Yu K, Lavine KJ, Ornitz DM, FGF9 regulates early hypertrophic chondrocyte differentiation and skeletal vascularization in the developing stylopod, Dev. Biol307 (2) (2007) 300–313. [PubMed: 17544391]

[13]. Hecht D, Zimmerman N, Bedford M, Avivi A, Yayon A, Identification of fibroblast growth factor 9 (FGF9) as a high affinity, heparin dependent ligand for FGF receptors 3 and 2 but not for FGF receptors 1 and 4, Growth Factors12 (3) (1995) 223–233. [PubMed: 8619928]

[14]. Santos-Ocampo S, Colvin JS, Chellaiah A, Ornitz DM, Expression and biological activity of mouse fibroblast growth factor-9, J. Biol. Chem271 (3) (1996) 1726–1731. [PubMed: 8576175]

[15]. Naski MC, Ornitz DM, FGF signaling in skeletal development, Front. Biosci3 (1998) d781–d794. [PubMed: 9683641]

[16]. Colvin JS, Bohne BA, Harding GW, McEwen DG, Ornitz DM, Skeletal overgrowth and deafness in mice lacking fibroblast growth factor receptor 3, Nat. Genet12 (4) (1996) 390–397. [PubMed: 8630492]

[17]. Behr B, Leucht P, Longaker MT, Quarto N, Fgf-9 is required for angiogenesis and osteogenesis in long bone repair, Proc. Natl. Acad. Sci. U. S. A107 (26) (2010) 11853–11858. [PubMed: 20547837]

[18]. Wallner C, Schira J, Wagner JM, Schulte M, Fischer S, Hirsch T, Richter W, Abraham S, Kneser U, Lehnhardt M, Behr B, Application of VEGFA and FGF-9 enhances angiogenesis, osteogenesis and bone remodeling in type 2 diabetic long bone regeneration, PLoS One10 (3) (2015), e0118823. .

[19]. Zhang X, Ibrahimi OA, Olsen SK, Umemori H, Mohammadi M, Ornitz DM, Receptor specificity of the fibroblast growth factor family. The complete mammalian FGF family, J. Biol. Chem281 (23) (2006) 15694–15700. [PubMed: 16597617]

[20]. Lin Y, Liu G, Wang F, Generation of an Fgf9 conditional null allele, Genesis44 (3) (2006) 150–154. [PubMed: 16496342]

[21]. Millard SM, Louie AM, Wattanachanya L, Wronski TJ, Conklin BR, Nissenson RA, Blockade of receptor-activated G(i) signaling in osteoblasts in vivo leads to site-specific increases in cortical and cancellous bone formation, J. Bone Miner. Res26 (4) (2011) 822–832. [PubMed: 20939063]

[22]. Kao RS, Abbott MJ, Louie A, O'Carroll D, Lu W, Nissenson R, Constitutive protein kinase A activity in osteocytes and late osteoblasts produces an anabolic effect on bone, Bone55 (2) (2013) 277–287. [PubMed: 23583750]

[23]. Wattanachanya L, Lu WD, Kundu RK, Wang L, Abbott MJ, O'Carroll D, Quertermous T, Nissenson RA, Increased bone mass in mice lacking the adipokine apelin, Endocrinology154 (6) (2013) 2069–2080. [PubMed: 23584856]

[24]. Abbott MJ, Roth TM, Ho L, Wang L, O'Carroll D, Nissenson RA, Negative skeletal effects of locally produced adiponectin, PLoS One10 (7) (2015), e0134290. .

[25]. Wang L, Hsiao EC, Lieu S, Scott M, O'Carroll D, Urrutia A, Conklin BR, Colnot C, Nissenson RA, Loss of Gi G-protein-coupled receptor signaling in osteoblasts accelerates bone fracture healing, J. Bone Miner. Res30 (10) (2015) 1896–1904. [PubMed: 25917236]

[26]. Kao R, Lu W, Louie A, Nissenson R, Cyclic AMP signaling in bone marrow stromal cells has reciprocal effects on the ability of mesenchymal stem cells to differentiate into mature osteoblasts versus mature adipocytes, Endocrine42 (3) (2012) 622–636. [PubMed: 22695986]

[27]. Feik SA, Thomas CD, Clement JG, Age-related changes in cortical porosity of the midshaft of the human femur, J. Anat191 (Pt 3) (1997) 407–416. [PubMed: 9418997]

[28]. Poole KE, Mayhew PM, Rose CM, Brown JK, Bearcroft PJ, Loveridge N, Reeve J, Changing structure of the femoral neck across the adult female lifespan, J. Bone Miner. Res25 (3) (2010) 482–491. [PubMed: 19594320]

[29]. Glatt V, Canalis E, Stadmeyer L, Bouxsein ML, Age-related changes in trabecular architecture differ in female and male C57BL/6J mice, J. Bone Miner. Res22 (8) (2007) 1197–1207. [PubMed: 17488199]

[30]. Mukherjee A, Larson EA, Klein RF, Rotwein P, Distinct actions of akt1 on skeletal architecture and function, PLoS One9 (3) (2014), e93040. .

[31]. Takei Y, Minamizaki T, Yoshiko Y, Functional diversity of fibroblast growth factors in bone formation, Int. J. Endocrinol2015 (2015) 729352.

[32]. Bottcher RT, Niehrs C, Fibroblast growth factor signaling during early vertebrate development, Endocr. Rev26 (1) (2005) 63–77. [PubMed: 15689573]

[33]. Thisse B, Thisse C, Functions and regulations of fibroblast growth factor signaling during embryonic development, Dev. Biol287 (2) (2005) 390–402. [PubMed: 16216232]

[34]. Li ZG, Mathew P, Yang J, Starbuck MW, Zurita AJ, Liu J, Sikes C, Multani AS, Efstathiou E, Lopez A, Wang J, Fanning TV, Prieto VG, Kundra V, Vazquez ES, Troncoso P, Raymond AK, Logothetis CJ, Lin SH, Maity S, Navone NM, Androgen receptor-negative human prostate cancer cells induce osteogenesis in mice through FGF9-mediated mechanisms, J. Clin. Invest118 (8) (2008) 2697–2710. [PubMed: 18618013]

[35]. Lu J, Dai J, Wang X, Zhang M, Zhang P, Sun H, Zhang X, Yu H, Zhang W, Zhang L, Jiang X, Shen SG, Effect of fibroblast growth factor 9 on the osteogenic differentiation of bone marrow stromal stem cells and dental pulp stem cells, Mol. Med. Rep11 (3) (2015) 1661–1668. [PubMed: 25435023]

[36]. Kawamura N, Kugimiya F, Oshima Y, Ohba S, Ikeda T, Saito T, Shinoda Y, Kawasaki Y, Ogata N, Hoshi K, Akiyama T, Chen WS, Hay N, Tobe K, Kadowaki T, Azuma Y, Tanaka S, Nakamura K, Chung UI, Kawaguchi H, Akt1 in osteoblasts and osteoclasts controls bone remodeling, PLoS One2 (10) (2007), e1058. .

[37]. Lai MS, Cheng YS, Chen PR, Tsai SJ, Huang BM, Fibroblast growth factor 9 activates akt and MAPK pathways to stimulate steroidogenesis in mouse leydig cells, PLoS One9 (3) (2014), e90243. .

[38]. Ohlsson C, Borjesson AE, Vandenput L, Sex steroids and bone health in men, Bonekey Rep. 1 (2012) 2. [PubMed: 23951414]

[39]. Manolagas SC, O'Brien CA, Almeida M, The role of estrogen and androgen receptors in bone health and disease, Nat. Rev. Endocrinol9 (12) (2013) 699–712. [PubMed: 24042328]

[40]. Colvin JS, Green RP, Schmahl J, Capel B, Ornitz DM, Male-to-female sex reversal in mice lacking fibroblast growth factor 9, Cell104 (6) (2001) 875–889. [PubMed: 11290325]

[41]. Nakae J, Kido Y, Accili D, Distinct and overlapping functions of insulin and IGF-I receptors, Endocr. Rev22 (6) (2001) 818–835. [PubMed: 11739335]

[42]. Vanderschueren D, Vandenput L, Boonen S, Lindberg MK, Bouillon R, Ohlsson C, Androgens and bone, Endocr. Rev25 (3) (2004) 389–425. [PubMed: 15180950]

[43]. Mason IJ, The ins and outs of fibroblast growth factors, Cell78 (4) (1994) 547–552. [PubMed: 8069907]

[44]. Rozenblatt-Rosen O, Mosonego-Ornan E, Sadot E, Madar-Shapiro L, Sheinin Y, Ginsberg D, Yayon A, Induction of chondrocyte growth arrest by FGF: transcriptional and cytoskeletal alterations, J. Cell Sci115 (Pt 3) (2002) 553–562. [PubMed: 11861762]

[45]. Mugniery E, Dacquin R, Marty C, Benoist-Lasselin C, de Vernejoul MC, Jurdic P, Munnich A, Geoffroy V, Legeai-Mallet L, An activating Fgfr3 mutation affects trabecular bone formation via a paracrine mechanism during growth, Hum. Mol. Genet21 (11) (2012) 2503–2513. [PubMed: 22367969]

[46]. Hendrix ND, Wu R, Kuick R, Schwartz DR, Fearon ER, Cho KR, Fibroblast growth factor 9 has oncogenic activity and is a downstream target of Wnt signaling in ovarian endometrioid adenocarcinomas, Cancer Res. 66 (3) (2006) 1354–1362. [PubMed: 16452189]

[47]. Teishima J, Yano S, Shoji K, Hayashi T, Goto K, Kitano H, Oka K, Nagamatsu H, Matsubara A, Accumulation of FGF9 in prostate cancer correlates with epithelial-to-mesenchymal transition and induction of VEGF-A expression, Anticancer Res. 34 (2) (2014) 695–700. [PubMed: 24511001]

[48]. Yin H, Frontini MJ, Arpino JM, Nong Z, O'Neil C, Xu Y, Balint B, Ward AD, Chakrabarti S, Ellis CG, Gros R, Pickering JG, Fibroblast growth factor 9 imparts hierarchy and vasoreactivity to the microcirculation of renal tumors and suppresses metastases, J. Biol. Chem290 (36) (2015) 22127–22142. [PubMed: 26183774]

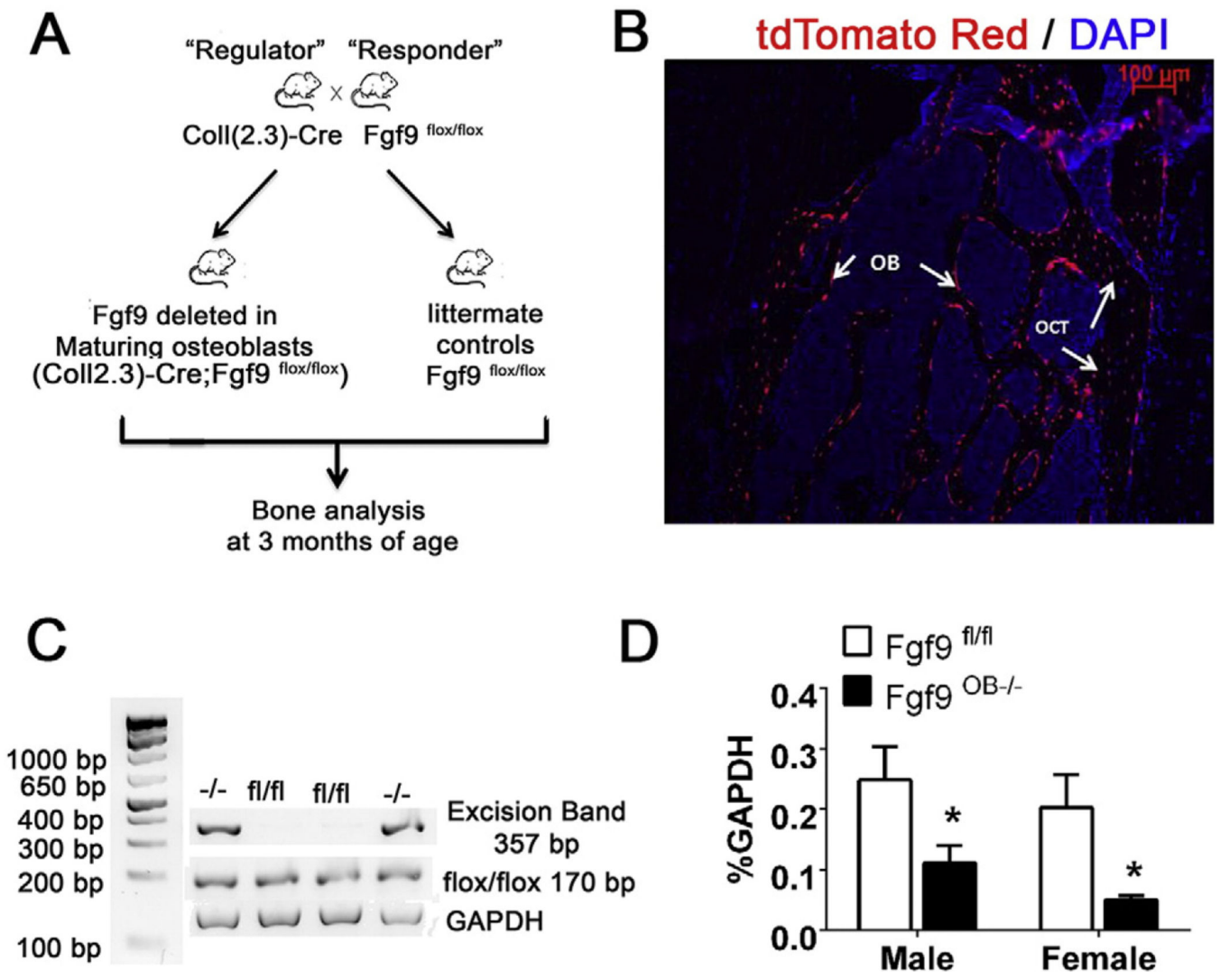

Fig. 1.

Establishment of a transgenic mouse model with the conditional deletion of Fgf9 in osteoblasts. A) Schematic showing the transgenic mouse model used in this study. B). The Cre recombinase is demonstrated to be expressed in osteoblasts (OBs) and osteocytes (OCTs) in adult Coll (2.3)-Cre; td/Tomato Red mice. C) Reverse transcription end point PCR demonstrated a successful excision of Fgf9 fragment in the RNA extract from the long bones of the Coll (2.3); Fgf9 $^{fl/fl}$ (Fgf9 $^{OB-/-}$) mice. D) Real time PCR assessment of the level of Fgf9 mRNA (relative to GAPDH) in the long bones of 3 months old Fgf9 $^{OB-/-}$ mice. *$p < 0.05$ vs. littermate controls (Fgf9 $^{fl/fl}$).

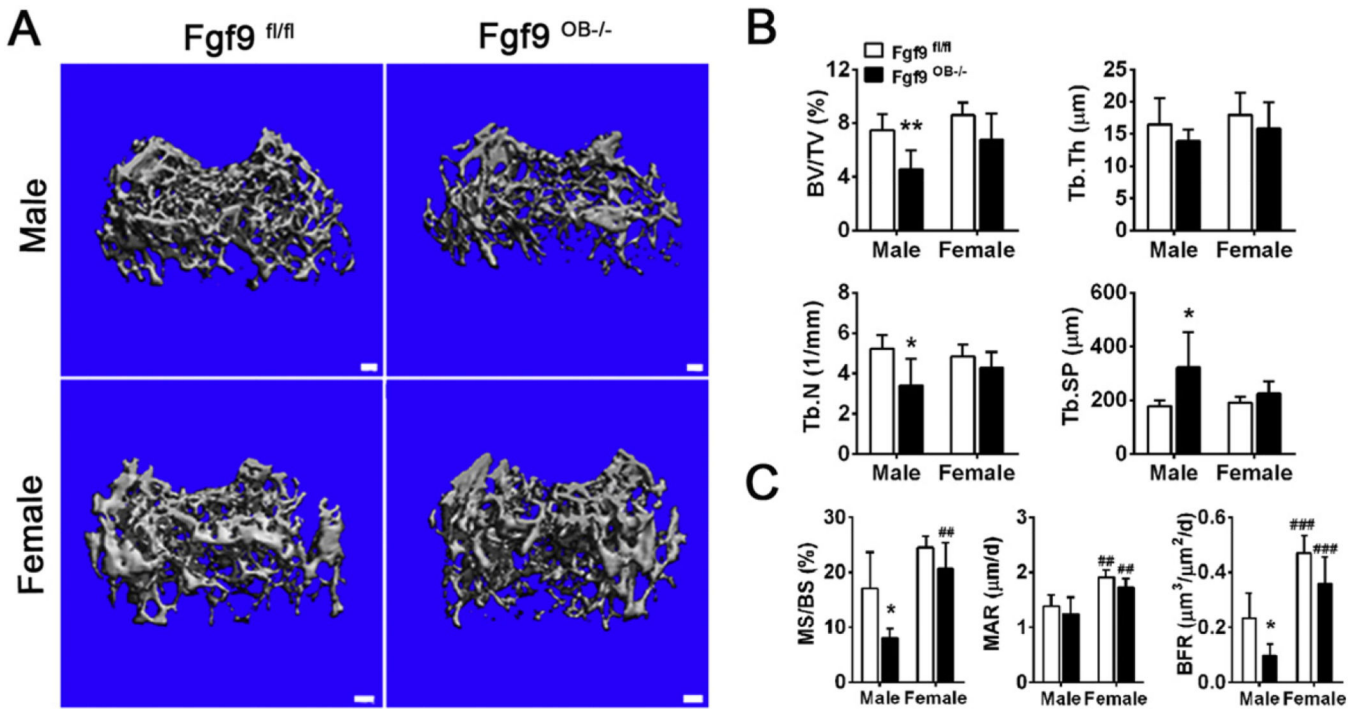

Fig. 2.

Assessment of cancellous bone mass at distal femur in the 3 month old male and female Fgf9 $^{OB-/-}$ mice. A). Representative μCT 3D reconstruction images of the distal femurs. B and C). Histomorphometry of cancellous bone at the distal femurs. BV, bone volume; TV, tissue volume; Tb.Th, trabecular thickness, Tb.Sp, trabecular separation; MS, mineralizing surface; MAR, mineral apposition rate, BFR, bone formation rate. ** $p < 0.01$, *$p < 0.05$ vs. the sex-matched littermate controls. ### $p < 0.001$, ## $p < 0.01$ vs. age-match Fgf9 $^{fl/fl}$ mice with the same genotype.

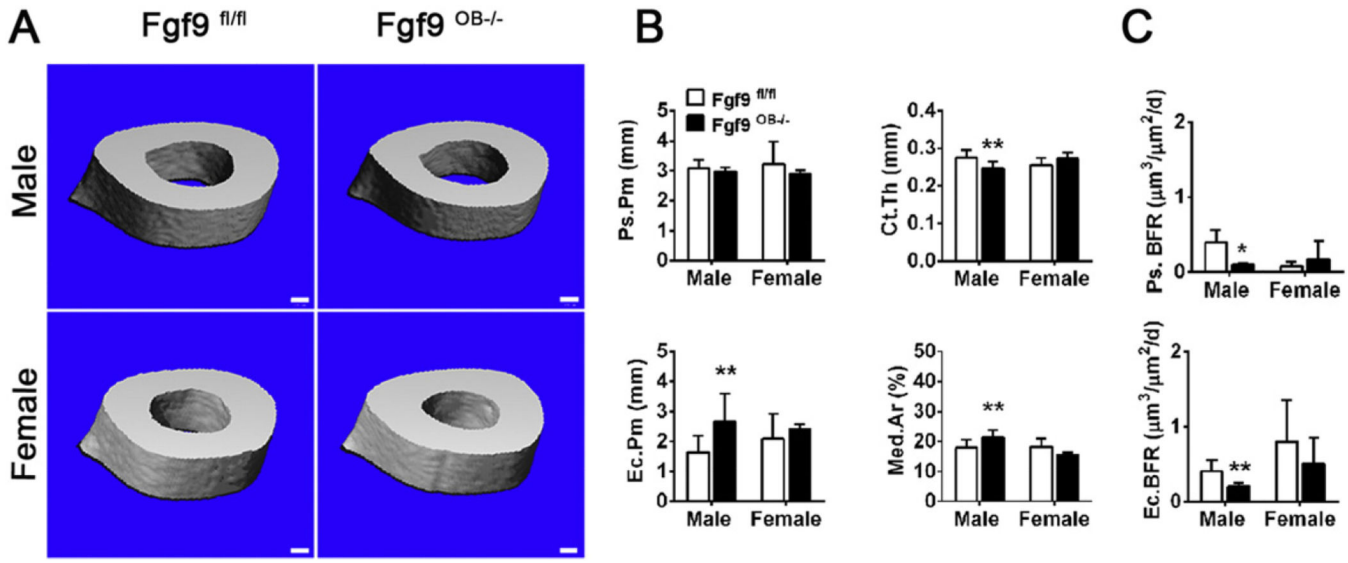

Fig. 3.

Assessment of cortical bone at tibio-fibular junction (TFJ) in the 3 month old male and female Fgf9 $^{OB-/-}$ mice. A). Representative 3D reconstruction images of μCT scan at the TFJ. B and C). Histomorphometry of cortical bone at the TFJ. Ps.Pm, periosteal perimeter; Ec.Pm, endosteal perimeter; Ct.Th, cortical thickness; Med.Ar, bone marrow area; Ps.BFR, periosteal bone formation rate, Ec.BFR, endosteal bone formation rate. ** $p < 0.01$, * $p < 0.05$ vs. the sex-matched littermate controls.

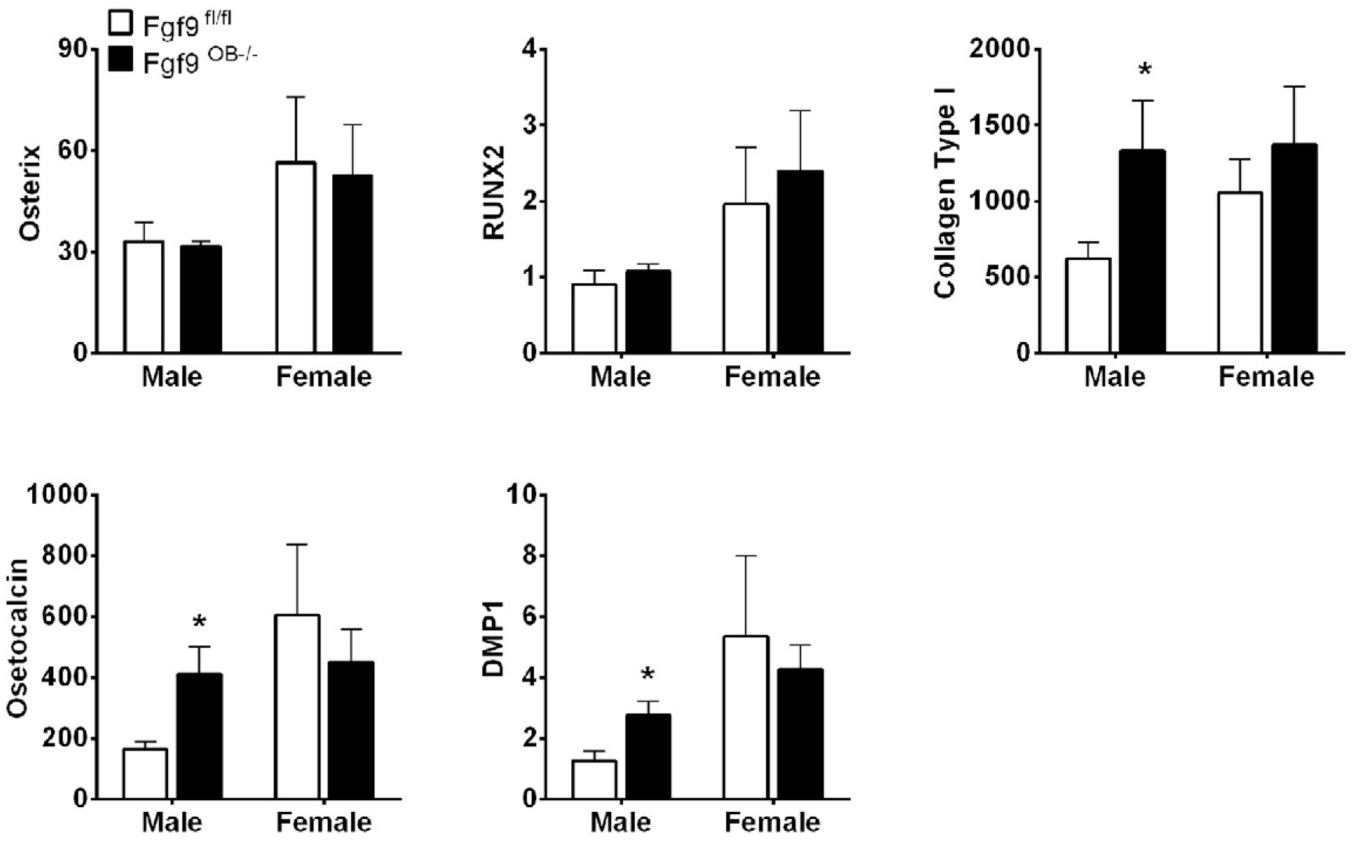

Fig. 4.

Determination of mRNA levels of osteogenic marker genes in the long bones of the 3 month old Fgf9 $^{OB-/-}$ mice. *$p < 0.05$ vs. the sex-matched littermate controls.

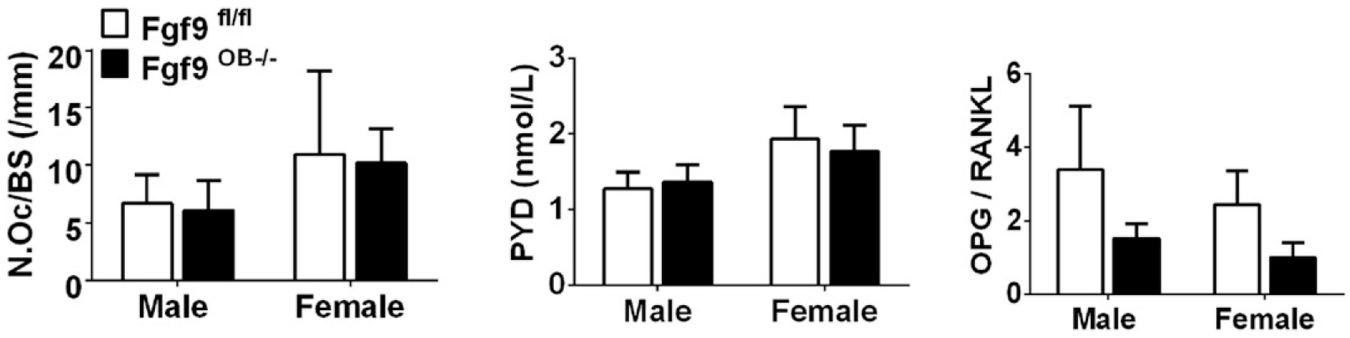

Fig. 5.

Assessment of bone resorption in the 3 months old Fgf9 $^{OB-/-}$ mice. N. OC, number of osteoclasts; BS, the length of bone surface. PYD, pyridinoline.

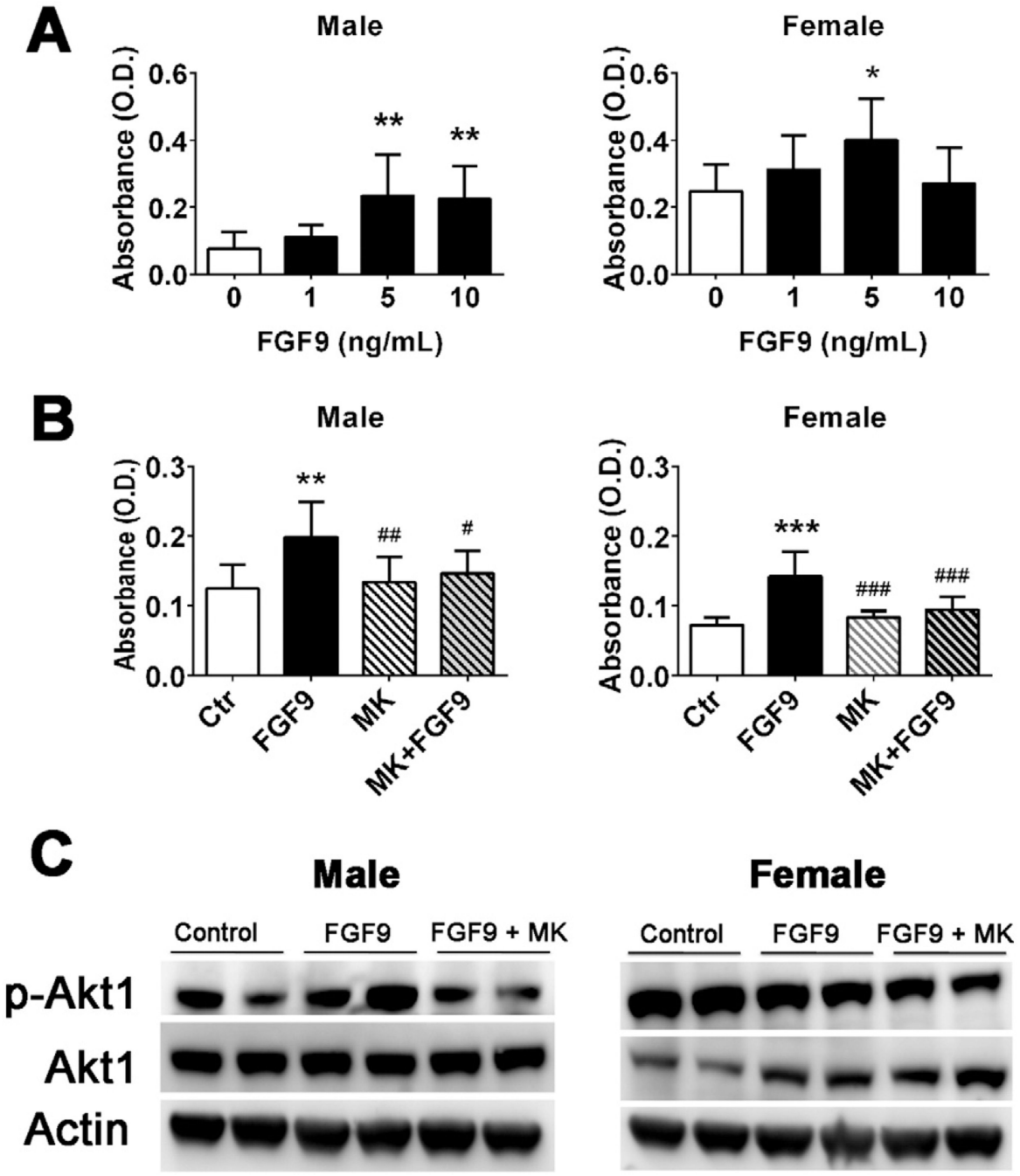

Fig. 6.

Effects of exogenous FGF9 on proliferation of the cultured bone marrow stromal cells (BMSCs). The BMSCs from wild type mouse were treated with exogenous FGF (5 ng/ml) for 24 h. A and B) Assessment of BMSC proliferation in the absence or presence of Akt inhibitor, MK-2206 (1 μM). Cell proliferation was determined by BrdU incorporation assay. C) Determination of Akt1 activation in BMSCs by FGF9 (5 ng/ml) using Western blots.

Table 1

µCT assessment of distal femur and tibiofibular junction in 3 month of Fgf9 $^{OB-/-}$ and littermate Fgf9 $^{fl/fl}$ mice.

Parameters	Male Fgf9 $^{fl/fl}$	Fgf9 $^{OB-/-}$	Female Fgf9 $^{fl/fl}$	Fgf9 $^{OB-/-}$
Distal femur				
BV/TV (%)	12.54 ± 2.09	9.252 ± 1.59 ***	13.29 ± 2.43	12.86 ± 1.40
Tb.N (1/mm)	5.059 ± 0.457	4.773 ± 0.537	4.873 ± 0.347	4.845 ± 0.595
Tb.Th (µm)	40.62 ± 2.63	36.18 ± 2.17 **	42.04 ± 4.35	43.00 ± 4.35
Tb.Sp (µm)	197.1 ± 18.4	212.5 ± 26.86	205.7 ± 17.46	208.8 ± 28.61
Tibio-fibular junction				
TV (mm^3)	0.3056 ± 0.025	0.2890 ± 0.016	0.2883 ± 0.018	0.2798 ± 0.039
BV (mm^3)	0.2116 ± 0.017	0.1965 ± 0.014 *	0.2101 ± 0.018	0.2030 ± 0.021
Ct.Th (mm)	0.2251 ± 0.014	0.2118 ± 0.017 *	0.2356 ± 0.019	0.2316 ± 0.011

Data are presented as Mean ± SD. BV, bone volume; TV, tissue volume; Tb.N, trabecular Number; Tb.Th, trabecular thickness; Tb.Sp, trabecular separation; Ct.Th, cortical thickness. Statistical analysis was determined by two-way ANOVA.

*** $p < 0.001$.

** $p < 0.01$.

* $p < 0.05$ vs. littermate control mice.